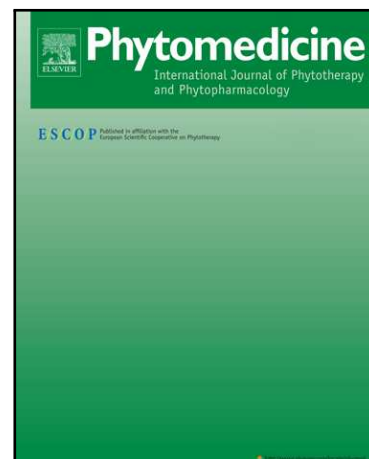


## Accepted Manuscript

Discovery of cardio-protective constituents of Gualou Xiebai  
Decoction, a classical traditional Chinese medicinal formula

Weiyang Zhang , Yang Yu , Lulu Yan , Chong Li , Jingyan Han ,  
Zifei Qin , Yi Dai , Zhihong Yao , Hua Zhou , Xinsheng Yao

PII: S0944-7113(18)30147-8  
DOI: [10.1016/j.phymed.2018.04.047](https://doi.org/10.1016/j.phymed.2018.04.047)  
Reference: PHYMED 52486



To appear in: *Phytomedicine*

Received date: 14 December 2017  
Revised date: 19 March 2018  
Accepted date: 16 April 2018

Please cite this article as: Weiyang Zhang , Yang Yu , Lulu Yan , Chong Li , Jingyan Han , Zifei Qin , Yi Dai , Zhihong Yao , Hua Zhou , Xinsheng Yao , Discovery of cardio-protective constituents of Gualou Xiebai Decoction, a classical traditional Chinese medicinal formula, *Phytomedicine* (2018), doi: [10.1016/j.phymed.2018.04.047](https://doi.org/10.1016/j.phymed.2018.04.047)

This is a PDF file of an unedited manuscript that has been accepted for publication. As a service to our customers we are providing this early version of the manuscript. The manuscript will undergo copyediting, typesetting, and review of the resulting proof before it is published in its final form. Please note that during the production process errors may be discovered which could affect the content, and all legal disclaimers that apply to the journal pertain.

**Discovery of cardio-protective constituents of *Gualou Xiebai Decoction*, a classical traditional Chinese medicinal formula**

Weiyang Zhang<sup>a,1</sup>, Yang Yu<sup>b,1</sup>, Lulu Yan<sup>a,c</sup>, Chong Li<sup>a</sup>, Jingyan Han<sup>c,d</sup>, Zifei Qin<sup>b</sup>, Yi Dai<sup>b</sup>, Zhihong Yao<sup>b,e</sup>, Hua Zhou<sup>a,\*</sup>, Xinsheng Yao<sup>a,b,\*</sup>

<sup>a</sup>Faculty of Chinese Medicine, Macau University of Science and Technology and State Key Laboratory of Quality Research in Chinese Medicine (Macau University of Science and Technology), Taipa, Macau, PR China

<sup>b</sup>College of Pharmacy, Jinan University, Guangzhou 510632, PR China

<sup>c</sup>Tasly Microcirculation Research Center, Peking University Health Science Center, Beijing 100191, PR China

<sup>d</sup>Department of Integration of Chinese and Western Medicine, School of Basic Medical Sciences, Peking University, Beijing 100191, PR China

<sup>e</sup>State key Laboratory of Drug Research, Shanghai Institute of Materia Medica, Chinese Academy of Sciences, Shanghai 201203, P.R. China

\* *Corresponding authors*

Prof. Hua Zhou, Faculty of Chinese Medicine, Macau University of Science and Technology and State Key Laboratory of Quality Research in Chinese Medicine (Macau University of Science and Technology), Taipa, Macau, PR China, Tel: +853-88972458 Fax: +853-28825886.

*E-mail address:* hzhou@must.edu.mo

Prof. Xinsheng Yao, Faculty of Chinese Medicine, Macau University of Science and Technology and State Key Laboratory of Quality Research in Chinese Medicine (Macau University of Science and Technology), Taipa, Macau, PR China; College of Pharmacy, Jinan University, 601 Huangpu Avenue, Guangzhou 510632, PR China. Tel. +86-20-85225849. Fax: +86-20-85221559,

*E-mail address:* tyaoxs@jnu.edu.cn

<sup>1</sup> Both authors contributed equally to this research.

ACCEPTED MANUSCRIPT

**ABSTRACT**

*Background:* Finding effective compounds of TCMs has always been the basis for achieving marker-based quality control which is currently most widely used quality control strategy. *Gualou Xiebai* Decoction (GLXB), a classical TCM formula, is recorded and proven as a therapy for curing coronary heart disease but the effective constituents are unidentified and the substantial basis of the therapeutic effects is not clear.

*Purpose:* The present research is an investigation on the chemistry of this formula aiming at finding and precisely identifying effective compounds.

*Study Design and Methods:* This research started with screening for effective fractions of GLXB by rat myocardial infarction model and H9c2 cell hypoxia/reoxygenation model, then compounds in effective fractions were isolated and identified by phytochemical and spectroscopic methods. The cardio-protective activities of the compounds were tested *in vitro* and one of the effective compounds was taken as example to investigate the mechanisms.

*Results:* The water-insoluble parts of GLXB were identified as effective parts in both *in vitro* and *in vivo* experiments. Systematic isolation of compounds in the effective fractions resulted in the isolation of 34 compounds including 7 new compounds, whereas 8 compounds were effective in protecting H9c2 cells against hypoxia/reoxygenation injury. One of the effective compounds, macrostemonoside P (MP) possibly exerted its effect by activating RISK pathway and attenuating apoptosis.

*Conclusion:* An array of effective constituents of GLXB were discovered, and discovery of these compounds contributed to elucidating the substantial basis for the therapeutic effects of this formula, and provides fundamentals for establishing Q-markers for further reliable quality control of GLXB.

*Keywords*

Traditional Chinese medicine formula, *Gualou Xiebai* Decoction, *Allii Macrostemonis Bulbus*, *Trichosanthis Fructus*, myocardial infarction, H9c2 cells

*Abbreviations*

AAR, areas-at-risk; Akt, protein kinase B; ANOVA, analysis of variance; Bax, Bcl-2-associated X protein; Bcl-2, B-cell lymphoma 2; CHD, coronary heart disease; DEPT, distortionless enhancement by polarization transfer; DMEM, Dulbecco's modified Eagle medium; DMSO, dimethylsulfoxide; eNOS, endothelial nitric oxide synthase; Erk1/2, extracellular signal-regulated kinases 1/2; FBS, fetal bovine serum; FITC/PI, fluorescein isothiocyanate / propidium iodide; GAPDH, glyceraldehyde-3-phosphate dehydrogenase; GLXB or GX, *Gualou Xiebai* Decoction;  $^1\text{H}$ - $^1\text{H}$  COSY, proton chemical shift correlation spectroscopy; H/R hypoxia/reoxygenation; HMBC,  $^1\text{H}$  detected heteronuclear multiple bond correlation; HPLC, high-performance liquid chromatography; HRESIMS, high-resolution electro-spray ionization mass spectroscopy; HRP, horseradish peroxidase; HSQC, heteronuclear singular quantum correlation; IA, infarct areas; IR, infrared spectroscopy, infrared spectrum; IRI, ischemia-reperfusion injury; KRB, Krebs-Ringer bicarbonate; LAD, left anterior descending branch; LV, left ventricle; MP, macrostemnoside P; MTT, methyl thiazolyl tetrazolium; NMR, nuclear magnetic resonance; NOESY, nuclear Overhauser effect correlation spectroscopy; OD, optical density; ODS, octadecyl silane; PI3K, phosphoinositide 3-kinase; Q-marker, quality marker; RISK pathway, reperfusion injury salvaging kinase pathway; SDS-HCl, sodium dodecyl sulfate-hydrochloric acid; SDS-PAGE, sodium dodecyl sulfate polyacrylamide gel electrophoresis; TCM, traditional Chinese medicine(s); TMS, tetramethyl silane; TTC, 2,3,5-triphenyl-2*H*-tetrazolium chloride; UHPLC-TOF-MS, ultra-high performance liquid chromatography-time-of-flight-mass spectroscopy; UV/vis, ultraviolet-visible spectroscopy.

## Introduction

*Gualou Xiebai* Decoction (GLXB), the alcoholic decoction of *Trichosanthis Fructus* and *Allii Macrostemonis Bulbus*, is one of the classical formulas originally recorded in “*Jin Kui Yao Lue*”. The indication of GLXB is depicted as “the symptoms of chest impediment and heart pain”, which corresponds with myocardial ischemia and coronary heart disease (CHD) in Western medicine (Zhu, 1999). CHD is the leading cause of death globally (WHO, 2007).

Great efforts and progress have been made on the pharmacological and chemical aspects of GLXB. Previously as depicted (Lei et al., 2013), the combination of *T. kirilowii* and *A. macrostemon* can improve the lesions of acute myocardium ischemia rats, similar results were afforded by several investigations. Ding *et al* investigated the preventive effect of GLXB against myocardial fibrosis (Ding et al., 2013) and their work also involved the screening for active parts of the formula and a preliminary chemical profiling (Ding, 2014). A study led by our team partially unveiled the chemical constituents of GLXB (He et al., 2002). Nevertheless, there has always been a pitfall elucidating the substantial basis for the therapeutic effects of this formula. Currently, effective constituents of GLXB are not sufficiently understood, and no quality control system has been proposed yet.

Establishing reliable quality control system for Chinese medicine formula is essential and needs chemical markers that can correctly reflect the safety and effectiveness of traditional Chinese medicines (TCMs) and can be qualitatively and quantitatively determined. These markers are usually bioactive chemical constituents of the formula. (Liu et al., 2017) The quality control system is questionable if quality control markers are not associated with the efficacy and/or safety. Therefore, a concept, “Q-marker”, was proposed to define such quality control markers (Liu et al., 2016).

In order to find and precisely identify effectiveness-related compounds as substantial basis for future establishment of Q-markers of GLXB, the present research involved screening of effective fractions of GLXB for preventing I/R-induced myocardial infarction, isolating compounds by phytochemical approaches and

identifying isolated compounds by spectroscopic methods. Then the effects of these compounds on hypoxia/reoxygenation (H/R) -induced cell death were investigated to find effective constituents.

## Materials and methods

### Plant materials

The samples of *T. Pericarpium* and *A. Macrostemonis Bulbus* were purchased from Handan Chinese Herbal Medicinal Materials Company (Handan, Hebei, China) and identified by Prof. Guang-xiong Zhou of Jinan University. Voucher specimens were deposited in the Institute of Traditional Chinese Medicine & Natural Products, Jinan University (No. JNU-TK-201503 and No. JNU-AM-201503), Guangzhou, China.

### Extraction and isolation

Dry *T. pericarpium* and *A. Macrostemonis Bulbus* were extracted by heat-reflux in 60% ethanol at a ratio of 1.5:1 (15 kg:10 kg). The extract (GX, a. 5 kg) was yielded by removing the solvents *in vacuo*, then loaded on an HP-20 macroporous resin column ( $\phi$  40×160 cm, Mitsubishi Chemical, Tokyo, Japan) and eluted with water, 30% ethanol and 95% ethanol successively, three fractions were yielded respectively, namely GX-1 (a. 4 kg, 80%), GX-2 (a. 780 g, 15.6%) and GX-3 (a. 240 g, 4.8%). UHPLC-TOF-MS chromatographs of GX, GX-1, GX-2 and GX-3 were established (Fig. S54). UHPLC-TOF-MS analysis was finished on an Agilent 6230 system with an Acquity™ BEH-C18 column ( $\phi$ 10×100 mm, 1.7  $\mu$ m). The procedures of systematic isolation and purification of compounds from GX-2 and GX-3 were depicted in the Supplementary Information. The purities of all compounds tested by <sup>1</sup>H-NMR and HPLC were > 90%.

### Spectroscopic determination

All NMR spectra were acquired on a Bruker AV 600 (Bruker, Co. Ltd, Bremen, German) using pyridine-*d*<sub>5</sub> or DMSO-*d*<sub>6</sub> as solvents and tetramethyl silane (TMS) as internal reference. High-resolution electro-spray ionization mass spectroscopies

(HRESIMS) were acquired on a Waters Synapt G2 mass spectrometer (Waters, Manchester, UK). Infrared spectra (IR) were acquired on a JASCO FT/IR-480 plus spectrometer (JASCO International Co. Ltd, Tokyo, Japan). The spectroscopic data were listed in the Tables 1 and 2 or described in Supplementary Information. The absolute configuration of saccharide moieties were determined by *o*-tolyl isothiocyanate derivatization and HPLC following a previously described method (Ni et al., 2017).

#### Rat myocardial ischemia reperfusion

Adult male Sprague-Dawley rats (240-260 g body weight) were kept in cages at room temperature ( $22 \pm 2$  °C) and constant humidity ( $40 \pm 5\%$ ) with regular 12 h day-night switch and constant fresh air. The animals were provided free access to water and food unless fasted. All procedures were in accordance to the guidelines of Commission of Animal Research of Peking University and approved by Peking University Institutional Animal Care and Use Committee (IACUC).

GX, GX-1, GX-2 and GX-3 were administrated at 4 g/kg, 3.06, 0.34 and 0.13 g/kg body weight by intragastric administration, respectively. The doses were calculated from the origin records in *Jin Kui Yao Lue* and confirmed by pre-experiments (data not shown, calculation and conversion of doses please see in the Supplementary Information). A course of 30 min ischemia and 90 min reperfusion was induced by left anterior descending branch (LAD) ligation following a reported protocol (Lin et al., 2013).

After 90 min reperfusion, LAD was ligated and 2 ml of 4% Evans blue in normal saline was injected through femoral vein then the heart was harvested immediately and cut into 1 mm cross sections. The cut sections were incubated in 0.375% 2,3,5-triphenyl-2*H*-tetrazolium chloride (TTC) phosphate buffer solution for 15 min at 37 °C. The images of the sections were recorded with a digital camera (DS-5M-U1, Nikon, Nanjing, China) connected to a stereoscope. Infarct areas were manifested by pale white color, ischemic but viable tissues (areas at-risk, AAR) were stained in red, and non-infarction areas were blue. AAR/LV (%) and IA/AAR (%) were calculated

and the average ratios of 5 slices were used to indicate the degree of myocardial infarction.

#### H9c2 cell hypoxia/reoxygenation assay

H9c2 myoblast cells (ATCC, Maryland, US) were cultured in Dulbecco's modified Eagle's medium (DMEM) with 10% fetal bovine serum (FBS), 100 U/ml penicillin and 100 µg/ml streptomycin (Gibco Invitrogen Corp., California, US) at 37 °C under normoxic condition (95% air / 5% CO<sub>2</sub>). When the confluence reached 80-90%, the cells were harvested by trypsinization (0.25% trypsin EDTA solution, Gibco Invitrogen Corp., California, US) and seeded in 96-well plates at 5000 cells/well. All tested compounds were dissolved in DMSO at 100 mM as stock solution. Thirty six h after seeding, the cells were pretreated by the compounds at 0.5, 5 and 50 µM for 1 h, then the cells were washed once with KRB (Krebs-Ringer Bicarbonate) culture buffer pre-balanced in nitrogen overnight and then given the compounds at the same concentrations (diluted with pre-balanced KRB culture buffer). The cells were deposited in a hypoxia chamber infused with nitrogen at 37 °C for 3 h. After hypoxia, the cells were given full DMEM and moved back to normoxic environment for 3 h' culture. For each well, 100 µl 0.5 mg/ml MTT (Sigma Aldrich Chemical Co., Missouri, US) dissolved in DMEM was added at the end of reoxygenation. After incubation at 37 °C for 4 h, 100 µl 10% sodium dodecyl sulfate-hydrochloric acid (SDS-HCl) was added in each well to dissolve the yielded formazan. Optical densities (OD) was determined after the formazan was fully dissolved (570 Abs / 610 Ref). Survival rates were calculated based on OD values and protection rates versus H/R group were calculated from survival rates.

#### Flow cytometry

Cells were stained with Annexin-V FITC/PI (fluorescein isothiocyanate/propidium iodide) apoptosis detection kit (BD Biosciences, California, US). H9c2 cells were seeded in a  $\phi$  3.5 cm culture dish. After overnight culture, the cells were treated by corresponding compounds and H/R following the same procedure in the 96-well plate assay. The cells were harvested by trypsinization and then treated with

the following protocol provided by the manufacturer. Briefly, after washing the harvested cells twice with ice-cold PBS, the cells were resuspended with the binding buffer at  $1 \times 10^6$  cells/ml, and 100  $\mu$ l of the suspension was collected and added with 5  $\mu$ l FITC labeled Annexin-V solution and 5  $\mu$ l PI solution. After incubating the cell suspension at room temperature in the dark for 15 min, the flow cytometry analysis was performed on a FACS Aria<sup>TM</sup> III Flow Cytometer (FACS Vantage-BD Sciences, Beckon Dickinson Company, California, US).

#### Western blotting

H9c2 cells were seeded in a  $\phi$  3.5 cm culture dish. After overnight culture, the cells were treated by the compound and H/R following the same procedure in the 96-well plate assay. The cells were washed twice with ice-cold PBS and lysed with RIPA buffer (Thermo Scientific, California, US). After a very short vortex, the lysed cells were kept in ice bath for 20 min. Then the lysates were centrifuged at 14,000 g for 15 min, the supernatant were collected and the contents of protein in the lysate were determined with Bio-Rad protein assay reagent (Bio-Rad, California, US). Samples equivalent to 60  $\mu$ g protein were loaded to 10% sodium dodecyl sulfate polyacrylamide gel electrophoresis (SDS-PAGE). After running, the proteins were electrotransferred to nitrocellulose filter membrane (PALL Corp., New York, US) and then incubated with 5% BSA solution at room temperature for 2 h. Primary antibodies of Bcl-2 (1:200, mouse, all antibodies were from Cell Signalling Technologies, Massachusetts, US), Bax (1:200, rabbit),  $\beta$ -actin (1:500, mouse), GAPDH (1:200, rabbit), phosphor-Erk 1/2 (1:200, rabbit), phosphor-Akt (1:200, rabbit), phosphor-PI3K (1:200, rabbit) and phosphor-eNOS (1:200, rabbit) were added to the membranes correspondingly and incubated at 4 °C overnight. Afterward, HRP-linked anti-rabbit or anti-mouse secondary antibodies were applied for 1.5 h at room temperature and HRP substrate solution was added to visualize the proteins. Photos were recorded on an Amersham Imager 600 System (G.E., Massachusetts, US) and the densities of bands were quantified by Image-J software.

#### Statistical analysis

One-way ANOVA with Tukey's multiple comparison test, significant levels: \*  $P < 0.05$ , \*\*  $P < 0.01$ , \*\*\*  $P < 0.001$ ,  $\alpha = 0.05$ , \* vs model group, # vs normal control.

## Results

### Active fractions of GLXB

An *in vivo* ischemia-reperfusion (I/R) model in rats was employed to examine the effect of GLXB and different fractions of GLXB. As shown in Fig. 1A and 1B, pretreatment of GX at 4 g/kg body weight can significantly reduce the infarction areas ( $P < 0.05$ ). When administrated at equivalent doses according to their proportions in the total extract (GX-1 3.06 g/kg, GX-2 0.34 g/kg and GX-3 0.13, *m/m*), GX-2 can significantly reduce the infarction size ( $P < 0.05$ ), while GX-3 showed some effects but weaker. The ischemic area of each group was similar.

Then the screening was conducted on *in vitro* model of H9c2 myoblast cell protection against H/R as well. The results indicated that the total extract (GX) and two water-insoluble fractions (GX-2 and GX-3) significantly increased cell survival rates in the MTT test (Fig. 1C). Taking both *in vivo* and *in vitro* results into consideration, GX, GX-2 and GX-3 were cardio-protective.

### Structure identification of new compounds

Compound **1** was obtained as white gum, and its molecular formula was assigned as  $C_{34}H_{58}O_{12}$  according to the HRESIMS ( $m/z$  627.3739  $[M-OCH_3]^+$ ,  $C_{33}H_{55}O_{11}$  calcd for 627.3744). The IR spectrum of **1** showed absorption bands for hydroxyl ( $3398\text{ cm}^{-1}$ ) and ketal ( $1079\text{ cm}^{-1}$ ) groups.  $^1\text{H-NMR}$  spectrum (Table 1) showed four methyl groups at  $\delta_{\text{H}}$  0.82 (3H, s, H<sub>3</sub>-18), 1.04 (3H, d, 5.1 Hz, H<sub>3</sub>-27), 1.17 (3H, d, 5.6 Hz, H<sub>3</sub>-21) and 1.37 (3H, s, H<sub>3</sub>-19), a methoxyl group at  $\delta_{\text{H}}$  3.26 (3H, s, 22-OCH<sub>3</sub>), and an anomeric proton signal at  $\delta_{\text{H}}$  4.84 (1H, d, 7.7 Hz, Glc-1'). In the  $^{13}\text{C-NMR}$  spectrum, a total of 34 carbon signals were observed. Except for the signals for a methoxyl and glucosyl groups, the remained 27 carbon resonances resolved as four methyls, 8 methylenes, 12 methines and three quaternary carbons, were characteristic of a C-27 steroidal aglycon moiety. Detailed comparison of 1D-NMR data of **1** with those of its analogue macrostemonoside M indicated that **1** was very likely a methoxylated

derivative of the latter (Chen et al., 2006).

Data assignment for **1** was conducted based on HSQC, HMBC and  $^1\text{H}$ - $^1\text{H}$  COSY spectra.  $\text{H}_3$ -19 ( $\delta_{\text{H}}$  1.37) showed HMBC correlations with C-1, C-5, C-9 and C-10, combined with sequential COSY correlations H-1/H-2/H-3/H<sub>2</sub>-4/H-5/H<sub>2</sub>-6/H<sub>2</sub>-7/H-8, indicating a A/B ring partial structure with four hydroxyls substituted at C-1,2,3,6. As other HMBC correlations of  $\text{H}_3$ -18/C-12, C-13, C-14, C-17 and  $\text{H}_3$ -21/C-17, C-20, C-22, together with COSY correlations of H<sub>2</sub>-11/H<sub>2</sub>-12 and H-15/H<sub>2</sub>-16/H-17/H-8, the assignment was established for C-E rings substructure. In addition, a spin system of H<sub>2</sub>-23/H<sub>2</sub>-24/H-25/H<sub>2</sub>-26 ( $\text{H}_3$ -27) and HMBC correlation of H-23/C-22 suggested the presence of a saturated C-22 side chain with an oxygenated group at C-26. Finally, the methoxyl and glucosyl groups were located at C-22 and C-26 as indicated by key HMBC correlations of 22-OCH<sub>3</sub>/C-22 and H<sub>2</sub>-26/C-1', respectively. The aglycone (**1a**) and monosaccharide were obtained after acid hydrolysis of **1**. Derivatization and HPLC experiments were used to identify the monosaccharide as a D-glucose. Furthermore, the  $\beta$ -configuration of anomeric proton was determined by a large coupling constant ( $J = 7.7$  Hz). The relative configuration of A and B rings was determined as the same as macrostemonoside M on the basis of NOESY correlations of  $\text{H}_3$ -19/H-5/H-6, H-2/H-9, H-1/H $_{\alpha}$ -11, H-1/H-2, H-2/H-3 and H-6/H-8. The 25*S* configuration of **1** was determined by the chemical shift deviation between H-26<sub>a</sub> and H-26<sub>b</sub>. Geminal proton resonances for H<sub>2</sub>-26 are more resolved in 25*S* isomers compared with 25*R* compounds, which was summarized as a criterion by Agrawal (Agrawal, 2005). In **1**, the difference ( $\delta_{\text{a}} - \delta_{\text{b}}$ ) was about 0.56 ppm near to the empirical deviation range of 25*S*-configuration ( $\delta_{\text{a}} - \delta_{\text{b}} > 0.57$  for 25*S* and  $\delta_{\text{a}} - \delta_{\text{b}} < 0.48$  for 25*R*). Meanwhile, peak strength  $916 > 898$  cm<sup>-1</sup> provided consistent result of 25*S*-configuration. Thus, **1** was identified as 22-methoxyl 25*S*-furostan-1 $\beta$ ,2 $\beta$ ,3 $\beta$ ,6 $\alpha$ ,26-pentol 26-*O*- $\beta$ -D-glucopyranoside.

Compound **2** was isolated as white gum. HRESIMS gave a quasi-molecular peak of  $[\text{M}+\text{Na}]^+$  at  $m/z$  683.3613 (C<sub>33</sub>H<sub>56</sub>O<sub>13</sub>Na calcd for 683.3619). IR absorptions of hydroxyl groups at 3396 cm<sup>-1</sup> and ketal C-O bond at 1077 cm<sup>-1</sup> were observed. The 1D-NMR and MS data indicated that **2** and **1** were very similar but differed at the

downfield shift of C-5 and absence of a methoxyl group. These were further supported by HMBC correlations of H<sub>3</sub>-19/C-1, C-5, C-9 and C-10, indicating a hydroxyl group at C-5. The absence of a methoxyl group signal indicated that C-22 was attached by a hydroxyl group. Similarly, the relative configurations of A and B rings in **2** were suggested to be the same as in **1**. The 25*R* configuration could be determined by the chemical shift deviation of H-26<sub>a</sub> and H-26<sub>b</sub>, whereas the IR spectra of the aglycon yielded a same result as 25*R* (917 < 899 cm<sup>-1</sup>). Therefore, compound **2** was identified as 25*R*-furostan-1β,2β,3β,5β,6α,26-hexol 26-*O*-β-D-glucopyranoside.

Also obtained as white gum, **3** had the same molecular formula of C<sub>33</sub>H<sub>56</sub>O<sub>13</sub> as compound **2** by HRESIMS ([M+Na]<sup>+</sup> *m/z* 683.3612, C<sub>33</sub>H<sub>56</sub>O<sub>13</sub>Na calcd for 683.3619). The NMR data of **3** showed high similarity to those of **2** except for slight differences of the proton chemical shifts of H<sub>2</sub>-26 and H<sub>3</sub>-27, indicating a possible configurational change at C-25. In **3**, the chemical shift deviation between H-26<sub>a</sub> and H-26<sub>b</sub> is 0.57, suggesting a 25*S* configuration. In conclusion, **3** was identified as 25*S*-furostan-1β,2β,3β,5β,6α,26-hexol 26-*O*-β-D-glucopyranoside.

Compound **4** was isolated as white powder. HRESIMS showed a quasi-molecular peak [M+H]<sup>+</sup> at *m/z* 625.3593, indicative of a molecular formula of C<sub>33</sub>H<sub>52</sub>O<sub>11</sub> (calcd for 625.3595). The 1D-NMR data of **4** showed a close resemblance to a known compound, macrostemonoside N (Chen et al., 2006), except for the presence of an olefinic carbons at C-20 and C-22. Thus, it was reasonable to infer that **4** was a dehydrated derivative of macrostemonoside, which was verified by HMBC correlations of H<sub>3</sub>-21/C-20, C-22, and a terminal double bond resonance at C-25(27). Thus, **4** was identified as 5β-furost-20(22), 25(27)-dien-1β,2β,3β,6α,26-pentol 26-*O*-β-D-glucopyranoside.

Compound **5** was isolated as white powder, the quasi-molecular peak at *m/z* 627.3742 ([M+H]<sup>+</sup>) was indicative of a molecular formula of C<sub>33</sub>H<sub>54</sub>O<sub>11</sub> ([M+H]<sup>+</sup> calcd for 627.3739). Except for two less olefinic carbon signals, other NMR data of **5** were very similar to **4**. The presence of H<sub>3</sub>-27 methyl peak in <sup>1</sup>H-NMR and HMBC correlations of H<sub>3</sub>-27/C-25, C-26 and H-25/C-23, C-24 indicated that C-25(27) was

saturated. In conclusion, the structure of **5** was defined as 25*S*-furost-20(22)-en-1 $\beta$ ,2 $\beta$ ,3 $\beta$ ,6 $\alpha$ ,26-pentol 26-*O*- $\beta$ -D-glucopyranoside.

Compound **6** was white powder when isolated, the quasi-molecular ion peak at  $m/z$  937.5008 was indicative of a molecular formula of C<sub>45</sub>H<sub>76</sub>O<sub>20</sub> ([M+H]<sup>+</sup> calcd for 937.5008). In the <sup>1</sup>H-NMR spectrum of **6**, methyl signals were seen as  $\delta_{\text{H}}$  0.85 (3H, s, H<sub>3</sub>-18), 1.03 (3H, d, 6.5 Hz, H<sub>3</sub>-27), 1.24 (3H, s, H<sub>3</sub>-19) and 1.32 (3H, d, H<sub>3</sub>-21), while three anomeric protons were present at  $\delta_{\text{H}}$  4.81, 4.95 and 5.36. The <sup>13</sup>C-NMR spectrum of **6** showed 45 signals including 27 carbons of the aglycon and 18 signals of three saccharide moieties. Acidic hydrolysates of **6** contained D-glucose and D-galactose in a ratio of 2:1 as determined by HPLC after derivatization.

Similarity between **6** and macrostemonoside P (Chen et al., 2007) was revealed by data assignment and comparison. Thereafter, differences were seen at the proton chemical shifts of H<sub>2</sub>-26 and H<sub>3</sub>-27. As the chemical shift deviation between H-26<sub>a</sub> and H-26<sub>b</sub> was 0.60 and H-27 was observed at  $\delta_{\text{H}}$  1.03, **6** was defined as a 25*S*-isomer of macrostemonoside P. Thus, compound **6** was identified as 25*S*-26-*O*- $\beta$ -D-glucosyl 5 $\beta$ -furostan-1 $\beta$ ,3 $\beta$ ,26-triol 3-*O*- $\beta$ -D-glucosyl (1 $\rightarrow$ 2)- $\beta$ -D-galactoside.

Compound **7** was isolated as white powder. HRESIMS showed an [M+H]<sup>+</sup> peak at  $m/z$  777.1872 (C<sub>35</sub>H<sub>36</sub>O<sub>20</sub> calcd for 777.1878). As displayed in ultraviolet-visible spectrum, typical absorption peaks of flavonoids were shown at 203, 267 and 345 nm. <sup>1</sup>H-NMR spectrum of **7** showed two sets of characteristic ABX aromatic protons [ $\delta_{\text{H}}$  7.17 (1H, d, 8.7 Hz, H-5'), 7.51 (1H, dd, 8.7, 2.2 Hz, H-6'), and 7.58 (1H, d, 2.2 Hz, H-2')] and [ $\delta_{\text{H}}$  6.66 (1H, d, 8.2 Hz, H-5'''), 7.14 (1H, dd, 8.2, 1.9 Hz, H-6''') and 7.24 (1H, d, 1.9 Hz, H-2''')], as well as a pair of meta-positioned protons on an aromatic ring [ $\delta_{\text{H}}$  6.36 (1H, br s, H-8) and 6.17 (1H, br s, H-6)]. Two anomeric protons were observed at [ $\delta_{\text{H}}$  5.54 (1H, d, 7.4 Hz, H-1'') and 4.83 (1H, d, 7.3 Hz, H-1''')], and a methoxyl group was seen at  $\delta_{\text{H}}$  3.68 (3H, s). <sup>13</sup>C-NMR spectrum of **7** showed 35 resonances in total including two secondary carbons, 18 tertiary carbons, 14 quaternary carbons, and a methoxyl group.

HMBC correlations of H-5'''/C-3''', C-4''', H-2'''/C-3''', C-4''', and H-2''', H-6'''/C=O were indicative of a benzoyl group with two oxygenated substituents, one

of which was a methoxyl group as verified by  $4'''$ -OCH<sub>3</sub>/C- $4'''$  correlation.

The rest 27 carbons belonged to a flavonoid aglycon and two hexoses. Two broadened singlets [ $\delta_H$  6.17 (1H, br s) and 6.36 (1H, br s)] were typical of H-6 and H-8 of 5,7-dihydroxyl A ring of flavonoid and the other ABX coupling system were arisen from the 3,4-disubstituted B ring. Chemical shifts of C-2 ( $\delta_C$  155.8) and C-3 ( $\delta_C$  133.9) were indicative of 3-OH, and the aglycon was defined as 3,5,7,3',4'-pentahydroxyl flavonoid, namely quercetin (Bendaikha et al., 2014; Xu et al., 2009). Meanwhile, two hexosyls were both identified as  $\beta$ -D-glucosyls.

Linkages between the aglycon and the glucosyls were established based on HMBC cross peaks of the anomeric protons and oxygenated carbons as H-1''/C-3 and H-1'''/C-3'. Whereas HMBC correlations of H<sub>2</sub>-6'''/C=O indicated that the 4-hydroxyl-3-methoxyl benzoyl was attached to C-6''' of 3'-O-glucosyl. Conclusively, **7** was identified as quercetin-3-O- $\beta$ -D-glucosyl-3'-O-6''-(4-hydroxyl-3-methoxyl benzoyl)- $\beta$ -D-glucoside.

Other compounds were known compounds identified based on their spectroscopic data, including 2,3,4,9-tetrahydro-1H-pyrido [3,4-b] indole-3-carboxylic acid (**8**) (He et al., 2003), macrostemonoside M (**9**), macrostemonoside N (**10**) (Chen et al., 2006), macrostemonoside G (**11**), macrostemonoside Q (**12**) (Chen et al., 2007), 26-[( $\beta$ -D-glucopyranosyl)oxy]-2 $\beta$ ,22-dihydroxy-5 $\beta$ -furostan-25(27)-en-3 $\beta$ -yl  $O$ - $\beta$ -D-glucopyranosyl-(1 $\rightarrow$ 2)-  $\beta$ -D-galactopyranoside (**13**), macrostemonoside J (**14**) (Peng et al., 1994), macrostemonoside P (**15**), macrostemonoside O (**16**) (Chen et al., 2007), timosaponin BII (**17**) (Guo et al., 2015), 25R-timosaponin BII (**18**), (2 $\alpha$ ,3 $\beta$ ,5 $\alpha$ )-27- $O$ -( $\beta$ -D-glucopyranosyl)-2,22-dihydroxyl furost-25-en-3-yl - $\beta$ -D-glucopyranosyl- (1 $\rightarrow$ 2)- $O$ - [ $\beta$ -D-glucopyranosyl-(1 $\rightarrow$ 3)] - $O$ - $\beta$ -D-glucopyranosyl- (1 $\rightarrow$ 4)-  $\beta$ -D-galactopyranoside (**19**), macrostemonoside R (**20**) (Chen et al., 2007), syringaresinol 4'- $O$ - $\beta$ -D-glucopyranoside (**21**) (Lami et al., 1991b), galangin 3- $O$ - $\beta$ -D-glucoside (**22**) (Kaouadji et al., 1988), luteolin (**23**) (Park et al., 2007), chrysoeriol 7- $O$ - $\beta$ -D-glucoside (**24**) (Fan et al., 2011b), quercetin 3- $O$ -L-ribose (**25**) (Kizu et al., 1995), luteoside (**26**) (Lami et al., 1991a),

isoquercetin (**27**) (Jin et al., 2009), quercitrin (**28**) (Lee et al., 2017), linarin (**29**) (Zhang et al., 2012), rutin (**30**) (Li et al., 2008), quercetin (**31**) (Chang et al., 2000), 5'-deoxy-5'- $\beta$ -methylsulphinyl-adenosine (**32**) (Wang and Lee, 1997), calycosin (**33**) (Cui et al., 1993) and davidigenin (**34**) (Siddaiah et al., 2006).

#### Anti-H/R effect of the compounds on H9c2 cells

A total of 18 out of all compounds were tested in the H9c2 cell hypoxia-reoxygenation assay. All tested compounds 1) were absorbed compounds or structural analogues of absorbed compounds (Lin, et al, 2018), 2) were abundant enough for finishing the tests ( $> 20$  mg obtained). Protection rates of the compounds were illustrated in Fig. 3 (mean  $\pm$  SD). As the most potent candidate, rutin (**30**) showed a protection rate of  $63.7 \pm 12.1\%$  at  $50 \mu\text{M}$ . While two other flavonoids, **25** and **27** were active as well ( $25.3 \pm 7.2\%$  and  $42.1 \pm 3.8\%$ , respectively). Other effective compounds, were all steroid saponins including **2**, **6**, **13**, **14** and **15**, among which the effect of **2** was significant at 5 and  $50 \mu\text{M}$  and **15** was significantly effective at 0.5, 5 and  $50 \mu\text{M}$  whereas others were significantly active at  $50 \mu\text{M}$  only.

#### Effects of macrostemnoside P on H/R-induced apoptosis and RISK pathway

As the effects and mechanisms of steroidal saponins were seldom investigated, macrostemnoside P (MP) was taken as an example to confirm the effects and investigate the mechanisms as it was the most potent saponin in this test and relatively abundant when isolated (27.7 mg). During IRI and H/R, apoptosis is an important cell death pathway. Cell apoptosis was analyzed by flow cytometry after Annexin-V FITC PI staining. As illustrated in Fig. 4A, the normal morphology of the cells collapsed after H/R and MP-treated cells mostly maintained their normal shape. Flow cytometric analysis indicated that H/R drastically increased FITC<sup>+</sup> cell proportion (mean 40.9%), whereas  $25 \mu\text{M}$  MP-treated cells showed decreased apoptotic proportions but the difference was not significant (29.5%), and  $50 \mu\text{M}$  group showed significant decrease (24.0%,  $P < 0.05$ ). Meanwhile, ratio of Bax/Bcl-2 was determined. Compared with the H/R group, MP groups showed a tendency of decrease in Bax/Bcl-2 ratios and the difference was significant in  $50 \mu\text{M}$  group ( $P <$

0.01).

The interaction between MP and phosphorylation activation of key proteins of RISK pathway was investigated. The data were illustrated as folds of normal group in Fig. 5. MP-treatment significantly increased phosphorylation of PI3K and eNOS at concentration of 50  $\mu\text{M}$  ( $P < 0.05$ ) and Akt at both 25 and 50  $\mu\text{M}$  ( $P < 0.05$ ) as shown in Fig. 5. Erk1/2 were activated when the cells underwent H/R and MP further promoted the phosphorylation of Erk1/2 to salvage the cells.

## Discussion

In this work, effective compounds in the effective fractions of GLXB were identified. The total extract and the less water-soluble fractions of GLXB were effective against myocardial infarction induced by ischemia-reperfusion *in vivo* and H/R-induced H9c2 cell death *in vitro*.

Investigation on the chemistry of active fractions yielded 34 compounds, including 18 steroidal saponins, 13 flavonoids and three compounds of other types (alkaloids and lignan). Steroidal saponin is the most important species of compounds in *A. macrostemon*. Approximately 50 steroidal saponins have been discovered from *A. macrostemon*, besides, *A. macrostemon* also contains sulfide volatile oil, lignans and alkaloids (Yao et al., 2016). Major constituents of *T. Fructus* (containing peels and seeds) are triterpenoid saponins (Akihisa et al., 1988; Akihisa et al., 1994), and flavonoids (Li et al., 2014) etc. However, since sugar, pectin and oil in the fruits and seeds can considerably interfere isolation and detection, meanwhile *T. Pericarpium* injection is approved for curing angina pectoris (Yao et al., 2017), *T. Pericarpium* was used instead of whole fruit in this research. The work of He (He, 2002) is the first report on active compounds in GLXB in which anticoagulative fractions were separated to yield 27 compounds and 12 of them were anticoagulative *in vitro*. Antithrombotic effect is an aspect in the prevention of atherosclerosis and CHD, so finding anticoagulative compounds in GLXB was a different view on this formula, and yielded different compounds.

In the H9c2 cell assay, flavonoids were mostly active including **25**, **27** and **30**, whereas other active components were steroid saponins including **2**, **6**, **13**, **14** and **15**.

The results indicated these compounds were effective constituents of GLXB for cardioprotective effects. During the occurrence of CHD, IRI and acute myocardial infarction compromise myocardium (Baliga, 2001; Morel et al., 2012), oxidative stress is one of the most important factors threatening cell survival (Frank et al., 2012). Flavonoids are potent naturally occurring anti-oxidants (Rice-Evans et al., 1996), the roles and mechanisms of flavonoids in alleviating IRI and countering oxidative stress have long been recognized (Cotelle, 2001). Steroidal saponins in *A. macrostemon* were highly diversified in structures, whereas their pharmacological effects were also diversified including protection against renal IRI (Manivannan et al., 2015), anti-coagulation, and cytotoxicity (Chen et al., 2009). Steroidal saponins from *A. macrostemon* were discovered as cardio-protective substances involved in this research, but they differed in cell-protective activity. Pitifully current results were not sufficient for a structure-activity relationship discussion which will be a good guidance for finding more efficacy-related substances in GLXB.

Moreover, this is the first to report the bioactivity and mechanism of macrostemonoside P. Macrostemonoside P possibly alleviated H/R-induced apoptosis, and the mechanism is associated with activating pro-survival protein kinases including PI3K, Akt and Erk1/2 to further activate eNOS. These proteins were termed reperfusion injury salvage kinase (RISK) pathway (Hausenloy and Yellon, 2004).

Reliable quality control system requires appropriate quality markers which 1) are components of the herbal materials, 2) have definite chemical structures and can be determined qualitatively and/or quantitatively, 3) are closely related to the efficacy and/or safety of the TCM herbs/formulas (Yang et al., 2017a, b). In the current research, as the effective constituents were obtained from effective fractions by phytochemical approaches and identified by comprehensive spectroscopic methods, the structures were fully elucidated including stereochemistry (Fig. 2). This approach can provide precise structural information and materials for pharmacological assays but not a full chemical profiling. Meanwhile, accurate evaluation of efficacy depends on appropriate pharmacological models. *In vivo* rat myocardial infarction model was employed in the screening for effective fractions and *in vivo* H9c2 cell H/R model

was employed in testing single compounds. Both are recognized as pharmacological models for the basic research of cardioprotection. Thus, as a linkage between compounds and therapeutic effects was built based on current results, these effective compounds are the substantial basis for the therapeutic effects of GLXB, at the same time potential Q-markers. Nevertheless, contents, detectability and measurability should be taken into consideration when establishing Q-markers based on substantial basis.

As the present research is limited to cardio-protective effects, while the effects of Chinese medicine formulae are mostly various and holistic, other aspects of this formula cannot be reflected from current results, for example, potential lipid-regulatory effects. Different roles of the component herbs have not been reflected from the effective compounds, either.

In conclusion, GLXB extract can significantly reduce infarction areas in rats undergone myocardial IRI, whereas water-insoluble parts of GLXB were the effective cardioprotective parts as revealed by both *in vivo* and *in vitro* experiments. Thereafter, isolation and structure elucidation of compounds from the active parts of GLXB provided a vision to the effective constituents of the formula, which are important fundamentals for establishing quality markers. *In vivo* assay indicated that effective constituents for cardioprotective effects are as follows: 25R-furostan-1 $\beta$ ,2 $\beta$ ,3 $\beta$ ,5 $\beta$ ,6 $\alpha$ ,26-hexol 26-O- $\beta$ -D-glucopyranoside (2), 25S-macrostemonoside P (6), 26-[( $\beta$ -D-glucopyranosyl)oxy]-2 $\beta$ ,22-dihydroxy-5 $\beta$ -furostan-25(27)-en-3 $\beta$ -yl O- $\beta$ -D-glucopyranosyl-(1 $\rightarrow$ 2)- $\beta$ -D-galactopyranoside (13), macrostemonoside J (14), macrostemonoside P (15), quercetin 3-O-L-riboside (25), isoquercetrin (27) and rutin (30), and these compounds are therefore potential Q-marker for establishment of reliable quality control system of GLXB products.

### Conflict of interest

The authors declare no conflict of interest.

**Acknowledgment**

The authors thank all the supports from Macao Science and Technology Development Fund (No. 035/2014/A1), the National Natural Science Foundation of China (81773880) and the State Key Laboratory of Drug Research (SIMM1705KF-17).

ACCEPTED MANUSCRIPT

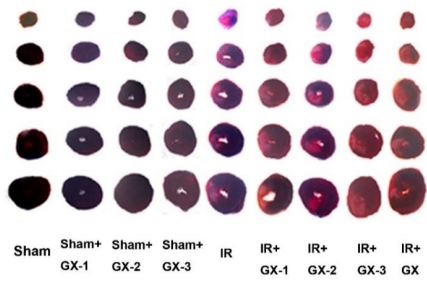
## References

- Agrawal, P.K., 2005. Assigning stereodiversity of the 27-Me group of furostane-type steroidal saponins via NMR chemical shifts. *Steroids* 70, 715-724.
- Akihisa, T., Tamura, T., Matsumoto, T., Eggleston, D.S., Kokke, W., Shimizu, N., 1988. Karounidiol [D: C-friedo-oleana-7, 9 (11)-diene-3 $\alpha$ , 29-diol] and its 3-O-benzoate: novel pentacyclic triterpenes from *Trichosanthes kirilowii*. X-Ray molecular structure of karounidiol diacetate. *J. Chem. Soc., Perkin Trans. 1*, 439-443.
- Akihisa, T., Yasukawa, K., Kimura, Y., Takido, M., Kokke, W.C., Tamura, T., 1994. 7-Oxo-10 $\alpha$ -Cucurbitadienol from the seeds of *Trichosanthes kirilowii* and its anti-inflammatory effect. *Phytochemistry* 36, 153-157.
- Baliga, R.R., 2001. Apoptosis in myocardial ischemia, infarction, and altered myocardial states. *Cardiol. Clin.* 19, 91-112.
- Bendaikha, S., Gadaut, M., Harakat, D., Magid, A., 2014. Acylated flavonol glycosides from the flower of *Elaeagnus angustifolia* L. *Phytochemistry* 103, 129-136.
- Chang, Y.C., Chang, F.R., Wu, Y.C., 2000. The constituents of *Lindera glauca*. *J. Chin. Chem. Soc.* 47, 373-380.
- Chen, H.F., Wang, G.H., Luo, Q., Wang, N.L., Yao, X.S., 2009. Two new steroidal saponins from *Allium macrostemon* Bunge and their cytotoxicity on different cancer cell lines. *Molecules* 14, 2246-2253.
- Chen, H.F., Wang, G.H., Wang, N.L., Yang, M.S., Wang, Z., Wang, X.W., Yao, X.S., 2007. New furostanol saponins from the bulbs of *Allium macrostemon* Bunge and their cytotoxic activity. *Die Pharmazie* 62, 544-548.
- Chen, H.F., Wang, N.L., Sun, H.L., Yang, B.F., Yao, X.S., 2006. Novel furostanol saponins from the bulbs of *Allium macrostemon* B. and their bioactivity on [Ca<sup>2+</sup>]<sup>i</sup> increase induced by KCl. *J. Asian Nat. Prod. Res.* 8, 21-28.
- Cotelle, N., 2001. Role of flavonoids in oxidative stress. *Curr. Top. Med. Chem.* 1, 569-590.
- Cui, B., Nakamura, M., Kinjo, J., Nohara, T., 1993. Chemical Constituents of *Astragalus Semen*. *Chem. Pharm. Bull. (Tokyo)* 41, 178-182.
- Ding, Y.F., 2014. Establishment and Application of Myocardial Fibrosis Cell Model Based on Endothelial-Mesenchymal Transition and the Application of *Gualou Xiebai Baijiutang*. Nanjing University of Chinese Medicine.
- Ding, Y.F., Peng, Y.R., Li, J., Shen, H., Shen, M.Q., Fang, T.H., 2013. Gualou Xiebai Decoction prevents myocardial fibrosis by blocking TGF-beta/Smad signalling. *J. Pharm. Pharmacol.* 65, 1373-1381.
- Fan, X.M., Chen, G., Su, S.S., Lu, X., Pei, Y.H., 2011a. Isolation and identification of constituents from fruit of *Trichosanthes kirilowii* Maxim. *Journal of Shenyang Pharmaceutical University* 12, 6.
- Fan, X.M., Chen, G., Su, S.S., Lu, X., Pei, Y.H., 2011b. Isolation and identification of constituents from fruit of *Trichosanthes kirilowii* Maxim. *Journal of Shenyang Pharmaceutical University* 12, 6.
- Frank, A., Bonney, M., Bonney, S., Weitzel, L., Koeppen, M., Eckle, T., 2012. Myocardial ischemia reperfusion injury: from basic science to clinical bedside, *Semin. Cardiothorac. Vasc. Anesth.* SAGE Publications Sage CA: Los Angeles, CA, pp. 123-132.
- Guo, J., Xu, C.H., Xue, R., Jiang, W.X., Wu, B., Huang, C.G., 2015. Cytotoxic activities of chemical constituents from rhizomes of *Anemarrhena asphodeloides* and their analogues. *Arch. Pharm. Res.* 38, 598-603.
- Hausenloy, D.J., Yellon, D.M., 2004. New directions for protecting the heart against ischaemia-reperfusion injury: targeting the Reperfusion Injury Salvage Kinase (RISK)-pathway. *Cardiovasc. Res.* 61, 448-460.
- He, X.J., 2002. The metabolites research of andrographolide in rats and the active constituents research of Gualou-Xiebai-Baijiu-Tang. Shenyang Pharmaceutical University.

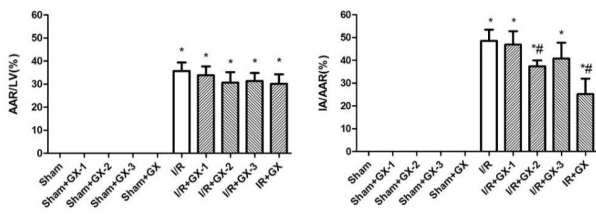
- He, X.J., Qiu, F., Shoyama, Y., Tanaka, H., Yao, X.S., 2002. Two New Steroidal Saponins from “Gualou-xiebai-baijiu-tang” Consisting of *Fructus trichosanthis* and *Bulbus allii macrostemi*. *Chem. Pharm. Bull. (Tokyo)* 50, 653-655.
- He, X.J., Qiu, F., Yao, X.S., 2003. The active constituents research of *Gualou Xiebai Baijiutang* (IV) nitrogen containing compounds and others. *Research and Exploration of Natural Products* 15, 9-12.
- Jin, H.Z., Chen, G., Li, X.F., Shen, Y.H., Yan, S.K., Zhang, L., Yang, M., Zhang, W.D., 2009. Flavonoids from *Rhododendron decorum*. *Chem. Nat. Compd.* 45, 85-86.
- Kaouadji, M., Ravel, P., Tissot, M., Creuzet, S., 1988. Novel methylated flavonols with unsubstituted B ring from *Platanus acerifolia* buds. *J. Nat. Prod.* 51, 353-356.
- Kizu, H., Shimana, H., Tomimori, T., 1995. Studies on the constituents of *Clematis* species. VI. The constituents of *Clematis stans* Sieb. et Zucc. *Chem. Pharm. Bull. (Tokyo)* 43, 2187-2194.
- Lami, N., Kadota, S., Kikuchi, T., Momose, Y., 1991a. Constituents of the roots of *Boerhaavia diffusa* L. III. Identification of Ca<sup>2+</sup> channel antagonistic compound from the methanol extract. *Chemical & pharmaceutical bulletin* 39, 1551-1555.
- Lami, N., Kadota, S., Kikuchi, T., Momose, Y., 1991b. Constituents of the roots of *Boerhaavia diffusa* L. III. Identification of Ca<sup>2+</sup> channel antagonistic compound from the methanol extract. *Chem. Pharm. Bull. (Tokyo)* 39, 1551-1555.
- Lee, H.E., Kim, J.A., Whang, W.K., 2017. Chemical Constituents of *Smilax china* L. Stems and Their Inhibitory Activities against Glycation, Aldose Reductase,  $\alpha$ -Glucosidase, and Lipase. *Molecules* 22, 451.
- Lei, Y., Huang, F., Han, L.T., Dan, H.X., Yan, B.W., Li, M.M., 2013. Influence of *Trichosanthes kirilowii* Maxim and *Allium macrostemon* Bge. on MAPK Signal Path against Rat Acute Myocardial Ischemia. *China Pharmaceuticals* 22, 11.
- Li, A.F., Sun, A.L., Liu, R.M., Zhang, Y.Q., Cui, J.C., 2014. An efficient preparative procedure for main flavonoids from the peel of *Trichosanthes kirilowii* Maxim. using polyamide resin followed by semi-preparative high performance liquid chromatography. *J. Chromatogr. B* 965, 150-157.
- Li, Y.L., Li, J., Wang, N.L., Yao, X.S., 2008. Flavonoids and a new polyacetylene from *Bidens parviflora* Willd. *Molecules* 13, 1931-1941.
- Lin, P., Qin, Z.F., Yao, Z.H., Wang, L., Zhang, W.Y., Yu, Y., Dai, Y., Zhou, H., Yao, X.S., Metabolites profile of Gualou Xiebai Baijiu decoction (a classical traditional Chinese medicine prescription) in rats by ultra-performance liquid chromatography coupled with quadrupole time-of-flight tandem mass spectrometry. *Under Review of Journal of Chromatography B*, Mar 2018.
- Lin, S.Q., Wei, X.H., Huang, P., Liu, Y.Y., Zhao, N., Li, Q., Pan, C.S., Hu, B.H., Chang, X., Fan, J.Y., Yang, X.Y., Wang, C.S., Liu, H.N., Han, J.Y., 2013. QiShenYiQi Pills® prevents cardiac ischemia-reperfusion injury via energy modulation. *Int. J. Cardiol.* 168, 967-974.
- Liu, C.X., Chen, S.L., Xiao, X.H., Zhang, T.J., Hou, W.B., Liao, M.L., 2016. A new concept on quality marker of Chinese materia medica: quality control for Chinese medicinal products. *Chin. Tradit. Herbal Drugs*, 1443-1457.
- Liu, C.X., Cheng, Y.Y., Guo, D.A., Zhang, T.J., Li, Y.Z., Hou, W.B., Huang, L.Q., Xu, H.Y., 2017. A new concept on quality marker for quality assessment and process control of Chinese medicines. *Chinese Herbal Medicines* 9, 3-13.
- Manivannan, J., Shanthakumar, J., Silambarasan, T., Balamurugan, E., Raja, B., 2015. Diosgenin, a steroidal saponin, prevents hypertension, cardiac remodeling and oxidative stress in adenine induced chronic renal failure rats. *RSC Adv.* 5, 19337-19344.
- Morel, O., Perret, T., Delarche, N., Labèque, J.-N., Jouve, B., Elbaz, M., Piot, C., Ovize, M., 2012. Pharmacological approaches to reperfusion therapy. *Cardiovasc. Res.* 94, 246-252.
- Ni, Y., Li, L., Zhang, W.Y., Lu, D., Zang, C.X., Zhang, D., Yu, Y., Yao, X.S., 2017. Discovery and LC-MS characterization of new crocins in *Gardeniae Fructus* and their neuroprotective potential. *J. Agric. Food Chem.* 65, 2936-2946.

- Park, Y.H., Moon, B.H., Lee, E.J., Lee, Y.S., Yoon, Y.D., Ahn, J.H., Lim, Y.H., 2007.  $^1\text{H}$  and  $^{13}\text{C}$  - NMR data of hydroxyflavone derivatives. *Magn. Reson. Chem.* 45, 674-679.
- Peng, J.P., Yao, X.S., Okada, Y., Okuyama, T., 1994. Further studies on new furostanol saponins from the bulbs of *Allium macrostemon*. *Chem. Pharm. Bull. (Tokyo)* 42, 2180-2182.
- Rice-Evans, C.A., Miller, N.J., Paganga, G., 1996. Structure-antioxidant activity relationships of flavonoids and phenolic acids. *Free Radic. Biol. Med.* 20, 933-956.
- Siddaiah, V., Rao, C.V., Venkateswarlu, S., Subbaraju, G.V., 2006. A concise synthesis of polyhydroxydihydrochalcones and homoisoflavonoids. 37, 841-846.
- Wang, P.H., Lee, S.S., 1997. Active chemical constituents from *Sauropus androgynus*. *J. Chin. Chem. Soc.* 44, 145-149.
- WHO, 2007. WHO international standard terminologies on traditional medicine in the western pacific region. Manila: WHO Regional Office for the Western Pacific.
- Xu, W.H., Jacob, M.R., Agarwal, A.K., Clark, A.M., Liang, Z.S., Li, X.C., 2009. Flavonol glycosides from the native American plant *Gaura longiflora*. *Heterocycles* 78, 2541-2548.
- Yang, W.Z., Zhang, Y.B., Wu, W.Y., Huang, L.Q., Guo, D.A., Liu, C.X., 2017a. Approaches to establish Q-markers for the quality standards of traditional Chinese medicines. *Acta Pharmaceutica Sinica B* 7, 439-446.
- Yang, W.Z., Zhang, Y.B., Wu, W.Y., Huang, L.Q., Guo, D.A., Liu, C.X., 2017b. Approaches to establish Q-markers for the quality standards of traditional Chinese medicines. *Acta pharmaceutica Sinica. B* 7, 439-446.
- Yao, Z., Wei, X., Weiwei, L., Chongbai, X., Ning, G., 2017. Gualoupi (Pericarpium Trichosanthis) injection in combination with convention therapy for the treatment of angina pectoris: a Meta-analysis. *J. Tradit. Chin. Med.* 37, 1-11.
- Yao, Z.H., Qin, Z.F., Dai, Y., Yao, X.S., 2016. Phytochemistry and pharmacology of *Allii Macrostemonis Bulbus*, a traditional Chinese medicine. *Chinese journal of natural medicines* 14, 481-498.
- Zhang, W.K., Xu, J.K., Zhang, L., Du, G.H., 2012. Flavonoids from the bran of *Avena sativa*. *Chinese Journal of Natural Medicines* 10, 110-114.
- Zhu, W.F., 1999. Standards for the diagnosis and therapy of diseases in Chinese internal medicine. Changsha, China.

A



B



C

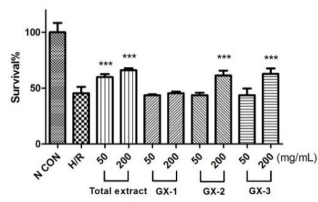


Fig. 1. The total extract of GLXB can prevent myocardial infarction after IRI and two of the fractions (GX-2 and GX-3) were effective as well. The protective effects were also shown in *in vitro* H/R model. (A) Evans blue and TTC stained tissues of each group after 30 min ischemia and 90 min reperfusion. White areas are infarction areas (IA), scarlet areas are area-at-risk (AAR). GX was administrated at 4 g/kg and the fractions were administrated at equivalent doses according to their proportions in the total extract (GX-1 3.06 g/kg, GX-2 0.34 g/kg and GX-3 0.13, m/m). (B) Calculated area ratio of each group, \* $P < 0.05$ , vs Sham, # $P < 0.05$  vs I/R. (C) Cell viability of H9c2 cells after treatment by 4 h hypoxia and 4 h reoxygenation and different extracts and fractions, \*\*\* $P < 0.001$ , vs H/R.

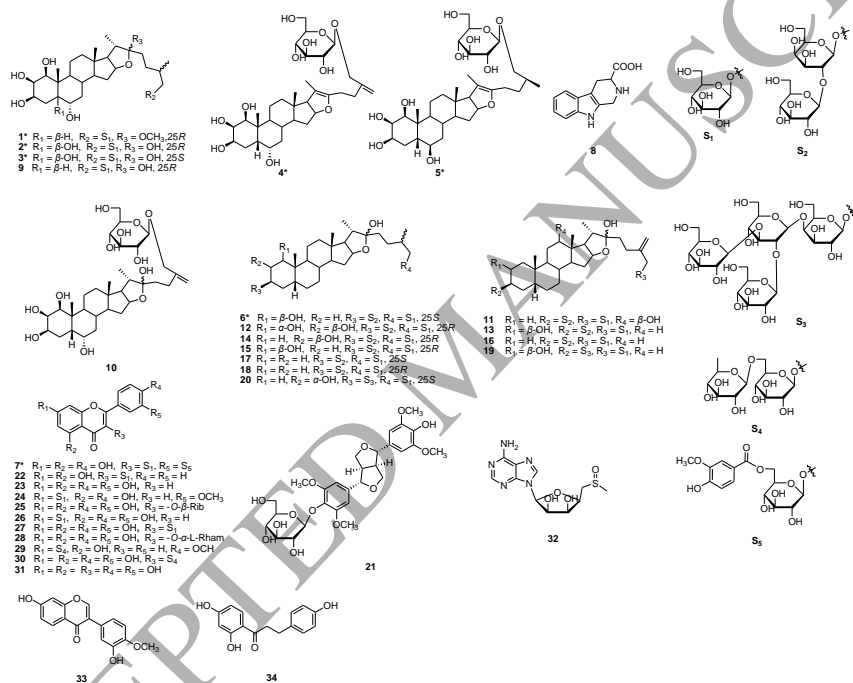


Fig. 2. Structures of compounds isolated from GLXB (starred numbers signify new compounds)

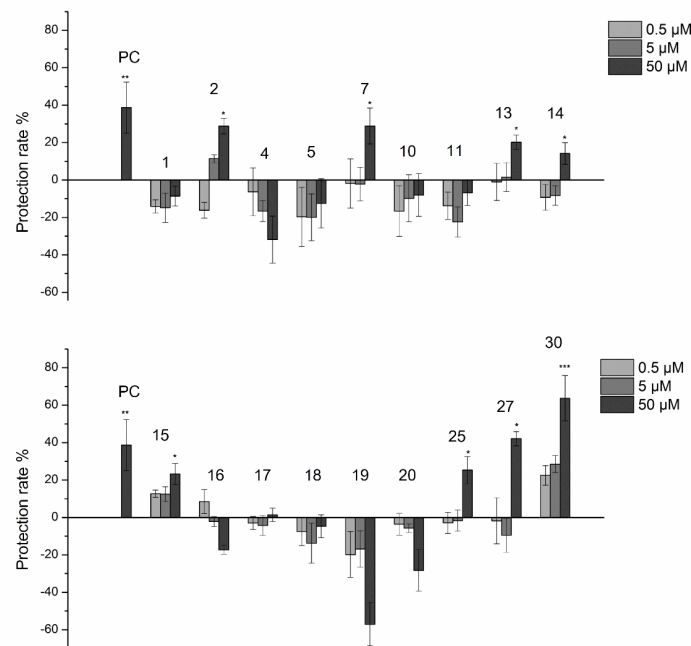


Fig. 3. Protective effects of GLXB compounds against H/R-induced cell death; adenosine was used as positive control (PC) at 50 μM; data were presented in protection rate (mean ± SD %, n = 3), \* $P < 0.05$ , \*\* $P < 0.01$ , \*\*\* $P < 0.001$ .

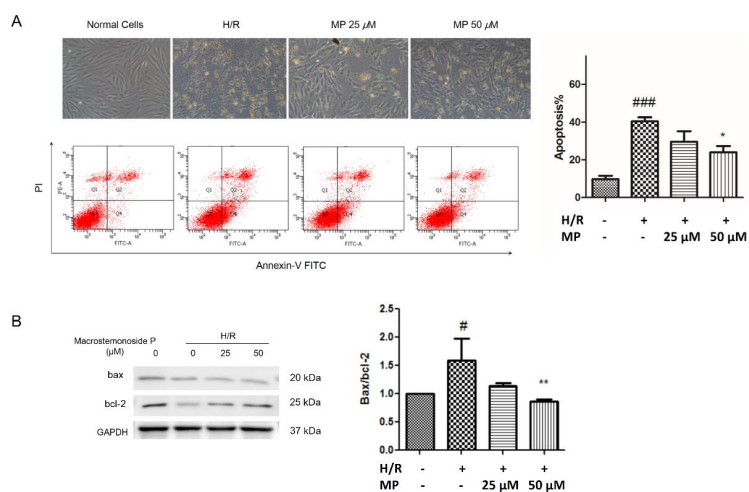


Fig. 4. MP alleviated H/R-induced apoptosis. (A) Microscopic photos and Annexin-V FITC/PI staining and flow cytometry: apoptotic percentages were illustrated (right, mean  $\pm$  SD %,  $n = 3$ ), \* $P < 0.05$ , \*\* $P < 0.01$ , \*\*\* $P < 0.001$ . (B) Representative Western blot photos of Bax and Bcl-2 in normal control, H/R, MP (25 and 50  $\mu$ M); ratios of Bax/Bcl-2 were shown in folds of normal control, (mean  $\pm$  SD,  $n = 3$ ), \* $P < 0.05$ , \*\* $P < 0.01$ , \*\*\* $P < 0.001$ , \* vs H/R, # vs normal control.

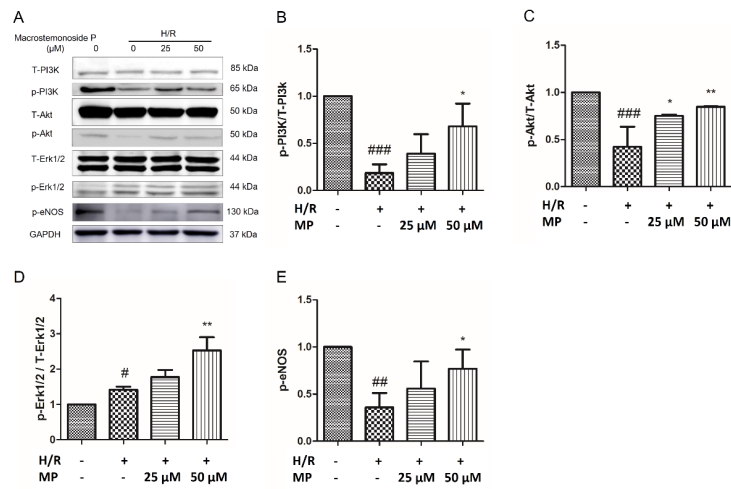
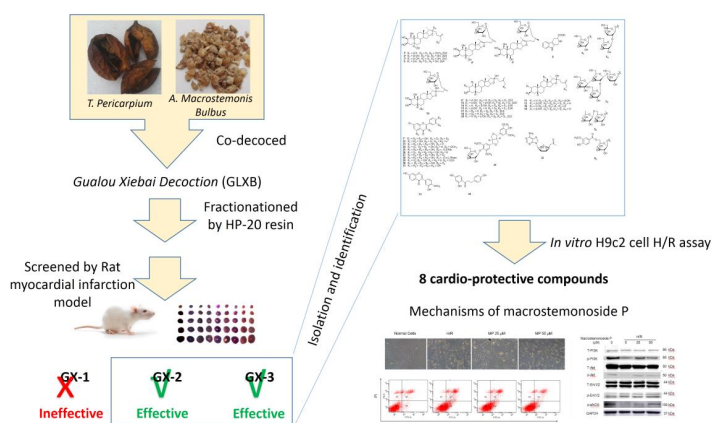


Fig. 5. MP activated RISK-pathway. (A) Representative Western blot photo of each group of cells; (B-E) Phosphorylation activation of PI3K, Akt, Erk1/2 and eNOS were illustrated as folds of normal control, (mean  $\pm$  SD, n = 3), \* $P$  < 0.05, \*\* $P$  < 0.01, \*\*\* $P$  < 0.001, # vs H/R, # vs normal control

graphic abstract

Table 1. NMR data of 1-5 (600 MHz for  $^1\text{H}$ -NMR and 150 MHz for  $^{13}\text{C}$ -NMR in pyridine- $d_5$ )

Positions	1		2		3		4		5	
	$\delta_{\text{C}}$	$\delta_{\text{H}}$	$\delta_{\text{C}}$	$\delta_{\text{H}}$	$\delta_{\text{C}}$	$\delta_{\text{H}}$	$\delta_{\text{C}}$	$\delta_{\text{H}}$	$\delta_{\text{C}}$	$\delta_{\text{H}}$
1	78.4	4.22	78.1	4.34, br s	78.2	4.34, br s	78.5	4.25	78.6	4.24
2	67.9	4.06	68.2	4.16	68.3	4.16	68.0	4.08	68.0	4.08
3	72.4	4.65	71.1	4.76	71.2	4.75	72.5	4.68	72.4	4.68
4	27.7	2.73, 2.06	32.5	2.99, br d (15.6) 2.37, br d (15.6)	32.5	3.00, br d (14.7), 2.38, dd (15.0, 2.2)	27.7	2.75, 2.11	27.7	2.76, 2.10
5	37.9	2.87	78.4	-	78.5	-	38.0	2.89	38.0	2.90
6	66.8	4.46	72.4	4.23	72.4	4.25	66.8	4.48	66.8	4.49
7	35.6	1.95, 1.48	37.0	2.03, 1.31	37.0	2.03, 1.33	35.7	1.95, 1.50	35.8	1.95, 1.49
8	35.0	1.77	34.3	1.84	34.5	1.86	34.8	1.73	34.8	1.74
9	41.7	1.38	45.6	1.31	45.6	1.34	41.6	1.38	41.6	1.38
10	43.1	-	46.4	-	46.4	-	43.2	-	43.2	-
11	21.2	1.40, 1.31	21.9	1.48, 1.43	21.9	1.50, 1.45	21.4	1.44, 1.33	21.4	1.45, 1.34
12	39.8	1.63, 1.06	40.1	1.68, 1.07	40.1	1.69, 1.08	39.8	1.68, 1.14	39.8	1.69, 1.14
13	41.1	-	41.0	-	41.1	-	43.6	-	43.7	-
14	56.0	1.19	56.0	1.16	56.0	1.17	54.4	1.00	54.4	1.00
15	32.2	2.05, 1.41	32.5	2.08, 1.47	32.5	2.07, 1.47	34.7	2.16, 1.49	34.5	2.16, 1.50
16	81.2	4.49	81.0	4.96, dd (14.6, 7.2)	81.0	4.97, dd (14.8, 7.3)	84.4	4.82	84.3	4.84
17	64.3	1.80	64.0	1.97	63.9	1.97	64.6	2.51	64.6	2.50
18	16.4	0.82, s	16.7	0.91, s	16.7	0.91, s	14.4	0.71, s	14.4	0.71, s
19	19.9	1.37, s	14.2	1.59, s	14.2	1.62, s	20.0	1.39, s	20.0	1.40, s

20	40.4	2.23	40.7	2.25	40.7	2.24	103.8	-	103.5	-
21	16.3	1.17, d (5.6)	16.5	1.33, d (6.6)	16.5	1.32, d (6.7)	11.7	1.62, s	11.7	1.61, s
22	112.6	-	110.7	-	110.7	-	151.7	-	152.4	-
23	30.9	1.93, 1.84	37.3	2.06	37.2	2.03	24.6	2.49, 2.40	23.6	2.25, 2.17
24	28.1	1.70, 1.44	28.5	2.04, 1.68	28.4	2.07, 1.69	31.0	2.50	31.4	1.85, 1.45
25	34.4	1.87	34.1	1.93	34.2	1.93	146.2	-	33.6	1.95
26	75.1	4.08, 3.52	75.3	3.95, 3.65	75.3	4.08, 3.49	71.7	4.62, 4.37	75.1	4.07, 3.49
27	17.5	1.04, d (5.1)	17.5	0.98, d (6.6)	17.5	1.04, d (6.6)	111.6	5.38, 5.07	17.1	1.04, d (6.7)
Glc-1'	105.0	4.84, d (7.7)	105.0	4.83, d (7.7)	105.2	4.83, d (7.7)	103.9	4.92, d (7.7)	105.2	4.84, d (7.8)
2'	75.2	4.04	75.4	4.04	75.4	4.04	75.1	4.07	75.1	4.02
3'	78.4	4.22	78.6	4.25	78.6	4.25	78.6	4.24	78.6	4.24
4'	71.6	4.22	71.8	4.22	71.8	4.23	71.7	4.25	71.7	4.24
5'	78.5	3.96	78.7	3.95	78.7	3.95	78.5	3.96	78.5	3.96
6'	62.8	4.56, br d (11.8), 4.38, dd (11.8, 4.5)	62.9	4.56, br d (11.6), 4.40, dd (11.6, 5.2)	62.9	4.56, dd (11.7, 2.3), 4.40, dd (11.7, 5.2)	62.8	4.56, br d (11.5), 4.40, dd (12.6, 6.1)	62.8	4.56, br d (11.8), 4.39, dd (11.6, 5.0)
22-OCH <sub>3</sub>	47.2	3.26, s								

Table 2. NMR data of compounds **6** (600 MHz for  $^1\text{H}$ -NMR and 150 MHz for  $^{13}\text{C}$ -NMR in pyridine- $d_5$ ) and **7** (600 MHz for  $^1\text{H}$ -NMR and 150 MHz for  $^{13}\text{C}$ -NMR in DMSO- $d_6$ )

6			6			7			7		
Positions	$\delta_{\text{C}}$	$\delta_{\text{H}}$	Positions	$\delta_{\text{C}}$	$\delta_{\text{H}}$	Positions	$\delta_{\text{C}}$	$\delta_{\text{H}}$	Positions	$\delta_{\text{C}}$	$\delta_{\text{H}}$
1	73.1	3.81	24	28.3	2.06, 1.69	2	155.8	-	Glc-1'''	101.9	4.83, d (7.3)
2	31.7	2.13, 1.79	25	34.4	1.94	3	133.9	-	2'''	74.9	3.32
3	72.2	4.68	26	75.2	4.09, 3.49	4	177.7	-	3'''	76.2	3.46
4	27.6	1.81	27	17.4	1.03, d (6.5)	5	161.5	-	4'''	70.8	3.18
5	30.8	2.38	C-26 Glc-1'	105.1	4.81, d (7.7)	6	99.5	6.17, br s	5'''	77.5	3.45
6	26.3	1.67, 1.11	2'	75.2	4.03	7	165.7	-	6'''	64.1	4.42, d (9.9), 4.07, dd (11.7, 7.5)
7	26.3	1.26, 0.98	3'	78.4	4.25	8	94.2	6.36, br s	6'''-C=O	165.7	-
8	35.7	1.54	4'	71.7	4.24	9	156.8	-	1'''	120.6	-
9	42.0	1.15	5'	78.6	3.94	10	103.9	-	2'''	112.6	7.24, d (1.9)
10	40.4	-	6'	62.8	4.56, 4.40	1'	124.9	-	3'''	147.6	-
11	21.0	1.21	C-3 Gal-1''	97.2	4.95, d (7.7)	2'	116.9	7.58, d (2.2)	4'''	151.9	-
12	40.2	1.70, 1.04	2''	80.1	4.62	3'	146.9	-	5'''	115.4	6.66, d (8.2)
13	40.9	-	3''	75.7	4.25	4'	147.9	-	6'''	123.4	7.14, dd (8.2, 1.9)
14	56.1	1.06	4''	70.3	4.53	5'	115.9	7.17, d (8.7), 7.51, dd (8.7, 2.2)	4'''-OCH <sub>3</sub>	55.8	3.68, s
15	32.4	2.00, 1.41	5''	77.2	4.05	6'	121.1	-			
16	81.1	4.96	6''	62.3	4.45	Glc-1''	101.1	5.54, d (7.4)			
17	63.9	1.93	Gal-Glc-1'''	105.5	5.36, d (7.7)	2''	74.4	3.29			
18	16.7	0.85, s	2'''	75.9	4.06	3''	76.8	3.31			
19	19.5	1.24, s	3'''	78.5	4.24	4''	70.1	3.20			
20	40.6	2.23	4'''	70.3	4.31	5''	77.6	3.36			
21	16.4	1.32, d (6.6)	5'''	78.7	3.49	6''	61.1	3.72, 3.50			
22	110.6	-	6'''	61.8	4.30						
23	37.1	2.08, 1.98									